

Direct observation of competition between superconductivity and charge density wave order in $\text{YBa}_2\text{Cu}_3\text{O}_{6.67}$

J. Chang^{1,2*}, E. Blackburn³, A. T. Holmes³, N. B. Christensen⁴, J. Larsen^{4,5}, J. Mesot^{1,2}, Ruixing Liang^{6,7}, D. A. Bonn^{6,7}, W. N. Hardy^{6,7}, A. Watenphul⁸, M. v. Zimmermann⁸, E. M. Forgan³ and S. M. Hayden⁹

Superconductivity often emerges in the proximity of, or in competition with, symmetry-breaking ground states such as antiferromagnetism or charge density waves^{1–5} (CDW). A number of materials in the cuprate family, which includes the high transition-temperature (high- T_c) superconductors, show spin and charge density wave order^{5–7}. Thus a fundamental question is to what extent do these ordered states exist for compositions close to optimal for superconductivity. Here we use high-energy X-ray diffraction to show that a CDW develops at zero field in the normal state of superconducting $\text{YBa}_2\text{Cu}_3\text{O}_{6.67}$ ($T_c = 67$ K). This sample has a hole doping of 0.12 per copper and a well-ordered oxygen chain superstructure⁸. Below T_c , the application of a magnetic field suppresses superconductivity and enhances the CDW. Hence, the CDW and superconductivity in this typical high- T_c material are competing orders with similar energy scales, and the high- T_c superconductivity forms from a pre-existing CDW environment. Our results provide a mechanism for the formation of small Fermi surface pockets⁹, which explain the negative Hall and Seebeck effects^{10,11} and the ' T_c plateau'¹² in this material when underdoped.

Charge density waves in solids are periodic modulations of conduction electron density. They are often present in low-dimensional systems such as NbSe_2 (ref. 4). Certain cuprate materials such as $\text{La}_{2-x-y}\text{Nd}_y\text{Sr}_x\text{CuO}_4$ (Nd-LSCO) and $\text{La}_{2-x}\text{Ba}_x\text{CuO}_4$ (LBCO) also show charge modulations that suppress superconductivity near $x = 1/8$ (refs 6,7). In some cases, these are believed to be unidirectional in the CuO_2 plane, and have been dubbed 'stripes'^{2,3}. There is now a mounting body of indirect evidence that charge and/or spin density waves (static modulations) may be present at high magnetic fields in samples with high T_c : quantum oscillation experiments on underdoped $\text{YBa}_2\text{Cu}_3\text{O}_y$ (YBCO) have revealed the existence of at least one small Fermi surface pocket^{9,10}, which may be created by a charge modulation¹¹. More recently, nuclear magnetic resonance (NMR) studies have shown a magnetic-field-induced splitting of the $\text{Cu}2\text{F}$ lines of YBCO (ref. 13). An important issue is the extent to which the tendency towards charge order exists in high- T_c superconductors^{2,3}.

Here we report a hard (100 keV) X-ray diffraction study, in magnetic fields up to 17 T, of a detwinned single crystal of

$\text{YBa}_2\text{Cu}_3\text{O}_{6.67}$ (with ortho-VIII oxygen ordering^{8,12}, $T_c = 67$ K and $p = 0.12$, where p is the hole concentration per planar Cu). We find that a CDW forms in the normal state below $T_{\text{CDW}} \approx 135$ K. The charge modulation has two fundamental wave vectors $\mathbf{q}_{\text{CDW}} = \mathbf{q}_1 = (\delta_1, 0, 0.5)$ and $\mathbf{q}_2 = (0, \delta_2, 0.5)$, where $\delta_1 \approx 0.3045(2)$ and $\delta_2 \approx 0.3146(7)$, with no significant field- or temperature-dependence of these values. The CDW gives rise to satellites of the parent crystal Bragg peaks at positions such as $\mathbf{Q} = (2 \pm \delta_1, 0, 0.5)$. Although the satellite intensities have a strong temperature and magnetic field dependence, the CDW is not field-induced and is unaffected by field in the normal state. Below T_c it competes with superconductivity, and a decrease of the CDW amplitude in zero field becomes an increase when superconductivity is suppressed by field. A very recent paper¹⁴ reports complementary resonant soft X-ray scattering experiments performed on $(\text{Y}, \text{Nd})\text{Ba}_2\text{Cu}_3\text{O}_{6+x}$ as a function of doping and in the absence of a magnetic field. The results are broadly in agreement with our zero field data.

Figure 1a,g shows scans through the $(2 - \delta_1, 0, 0.5)$ and $(0, 2 - \delta_2, 0.5)$ positions at $T = 2$ K. Related peaks were observed at $(2 + \delta_1, 0, 0.5)$ and $(4 - \delta_1, 0, 0.5)$ (see Supplementary Fig. S3). The incommensurate peaks are not detected above 150 K (Fig. 1c). From the peak width we estimate that the modulation has an in-plane correlation length $\xi_a \approx 95 \pm 5$ Å (at 2 K and 17 T—see Methods). The existence of four similar in-plane modulations $(\pm\delta_1, 0)$ and $(0, \pm\delta_2)$ indicates that the modulation is associated with the (nearly square) CuO_2 planes rather than the CuO chains. The present experiment cannot distinguish between $1 - \mathbf{q}$ and $2 - \mathbf{q}$ structures, that is, we cannot tell directly whether modulations along the a and b directions co-exist in space or occur in different domains of the crystal. However, Bragg peaks from the two CDW components have similar intensities and widths (Fig. 1b,g) despite the orthorhombic crystal structure, which breaks the symmetry between them. This suggests that \mathbf{q}_1 and \mathbf{q}_2 are coupled, leading to the co-existence of multiple wave vectors, as seen in other CDW systems such as NbSe_2 (ref. 4). The scan along the c^* direction in Fig. 1d has broad peaks close to $l = \pm 0.5$ reciprocal lattice units (r.l.u.), indicating that the CDW is weakly correlated along the c direction, with a correlation length ξ_c of approximately 0.6 lattice units.

¹Institut de la Matière Complexe, Ecole Polytechnique Fédérale de Lausanne (EPFL), CH-1015 Lausanne, Switzerland, ²Paul Scherrer Institut, Swiss Light Source, CH-5232 Villigen PSI, Switzerland, ³School of Physics and Astronomy, University of Birmingham, Birmingham, B15 2TT, UK, ⁴Department of Physics, Technical University of Denmark, DK-2800 Kongens Lyngby, Denmark, ⁵Laboratory for Neutron Scattering, Paul Scherrer Institut, CH-5232 Villigen PSI, Switzerland, ⁶Department of Physics and Astronomy, University of British Columbia, Vancouver, Canada, ⁷Canadian Institute for Advanced Research, Toronto, Canada, ⁸Hamburger Synchrotronstrahlungslabor (HASYLAB) at Deutsches Elektronen-Synchrotron (DESY), 22603 Hamburg, Germany, ⁹H. H. Wills Physics Laboratory, University of Bristol, Bristol, BS8 1TL, UK. *e-mail: johan.chang@epfl.ch.

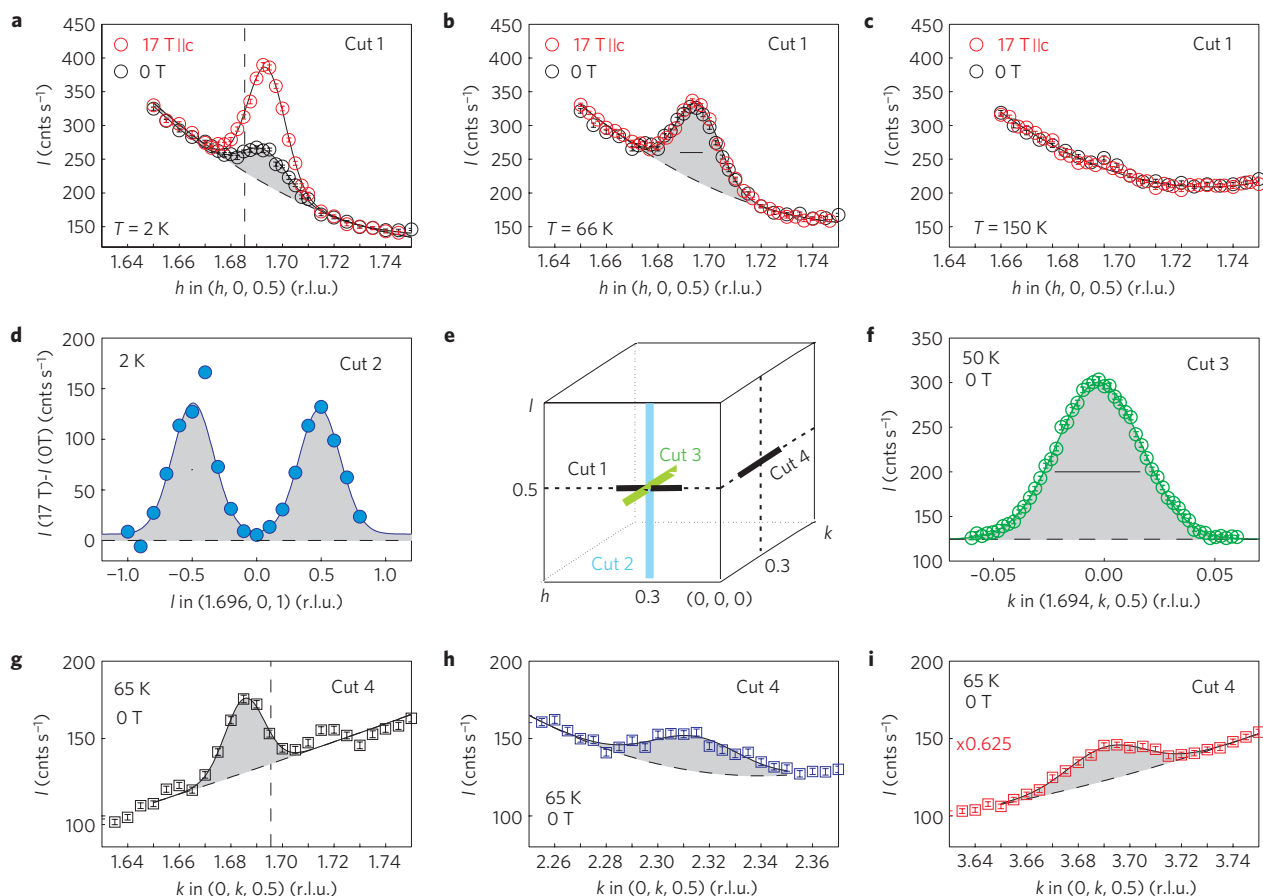


Figure 1 | Incommensurate charge-density-wave order. Diffracted intensity in reciprocal space $\mathbf{Q} = (h, k, l) = h\mathbf{a}^* + k\mathbf{b}^* + l\mathbf{c}^*$ where $\mathbf{a}^* = 2\pi/a$, $\mathbf{b}^* = 2\pi/b$ and $\mathbf{c}^* = 2\pi/c$, with lattice parameters $a = 3.81 \text{ \AA}$, $b = 3.87 \text{ \AA}$ (Supplementary Fig. S1), $c = 11.72 \text{ \AA}$. Four different scans in reciprocal space, projected into the first Brillouin zone, are shown schematically in **e**. **a–c**, Scans along $(h, 0, 0.5)$ for temperatures and magnetic fields (applied along the crystal c -direction) as indicated. An incommensurate lattice modulation, peaked at $(2 - \delta_1, 0, 0)$, where $\delta_1 = 0.3045(2)$, emerges as the temperature is lowered below 135 K. The intensity of the satellite in **b** is of the order 2×10^{-6} weaker than the $(2, 0, 0)$ reflection. This becomes field-dependent below the zero-field superconducting transition temperature $T_c = 67 \text{ K}$. The full-width half-maximum instrumental resolution is shown by horizontal lines in **b, f**. By deconvolving the resolution from the Gaussian fits to the data taken at 17 T and 2 K, an h -width of $\sigma_a = 6.4 \times 10^{-3}$ r.l.u. corresponding to a correlation length $\xi_a = 1/\sigma_a$ of $95 \pm 5 \text{ \AA}$ was found (see Methods). **d**, The field-induced signal $I(17 \text{ T}) - I(0 \text{ T})$ at $T = 2 \text{ K}$ is modulated along $(1.695, 0, l)$ and peaks at approximately $l = \pm 0.5$. **f**, Scan along $(1.695, k, 0.5)$. The poor resolution along the k -direction did not allow accurate determination of the width along $(1.695, k, 0.5)$, but we estimate a value of 0.01 r.l.u., comparable to that along $(h, 0, 0.5)$, indicating similar coherence lengths along a - and b -axis directions. **g–i**, Scans along $(0, k, 0.5)$. Incommensurate peaks are found in several Brillouin zones, for example, at positions $\mathbf{Q} = (0, 2 \pm \delta_2, 0.5)$ and $(0, 4 - \delta_2, 0.5)$, where $\delta_2 = 0.3146(7)$, see also Supplementary Fig. S3. The vertical dashed line in **g** indicates δ_1 whereas the line in **a** indicates δ_2 . The lattice modulation was fitted to a Gaussian function (solid lines in **a–d, f–i**) on a background (dashed lines) modelled by a second-order polynomial. Error bars are determined by counting statistics.

In zero field, the intensity of the CDW Bragg peak (Fig. 2) grows on cooling to T_c , below which it is partially suppressed. For $T > T_c$, a magnetic field applied along the c direction has no effect. Below T_c it causes an increase of the intensity of the CDW signal (Figs 1a and 2). At $T = 2 \text{ K}$, the intensity grows with applied magnetic field (Fig. 2b) and shows no signs of saturation up to 17 T. The magnetic field also makes the CDW more long-range ordered (Fig. 2c). In zero magnetic field, the q -width varies little with temperature. However, below T_c in a field, the CDW order not only becomes stronger, but also becomes more coherent, down to a temperature T_{cusp} below which the intensity starts to decrease (Figs 2 and 4). All of this is clear evidence for competition between CDW and superconducting orders.

Non-resonant X-ray diffraction is sensitive to modulations of charge density and magnetic moments. In our case, the expected magnetic cross-section is several orders of magnitude smaller than our observed signal, which must therefore be due to charge scattering. NMR measurements on a sample of the same composition as

ours¹³ indicate that the CDW is not accompanied by magnetic order, and this is confirmed by soft X-ray measurements, which would also be sensitive to fluctuating order¹⁴. Charge density modulations in solids will always involve both a modulation of the electronic charge and a periodic displacement of the atomic positions¹⁵. We are more sensitive to the atomic displacements than to the charge modulation because ions with large numbers of electrons (as in YBCO) dominate the scattering (see Supplementary Information).

NMR data¹³ suggest that CDW order only appears below $T \approx 67 \text{ K}$ and $H > 9 \text{ T}$, whereas with X-rays we observe CDW order in zero field up to 135 K. This apparent discrepancy may arise from differing timescales of various probes (see Supplementary Information for further discussion). X-ray diffraction experiments are usually interpreted as measuring the static order of a given structure, but, if performed with wide energy acceptance, are also sensitive to short-lived structures. Thus, it is possible that the observed CDW is quasi-static and only frozen on the NMR timescale ($\approx 3 \text{ ns}$) at high fields and lower temperatures.

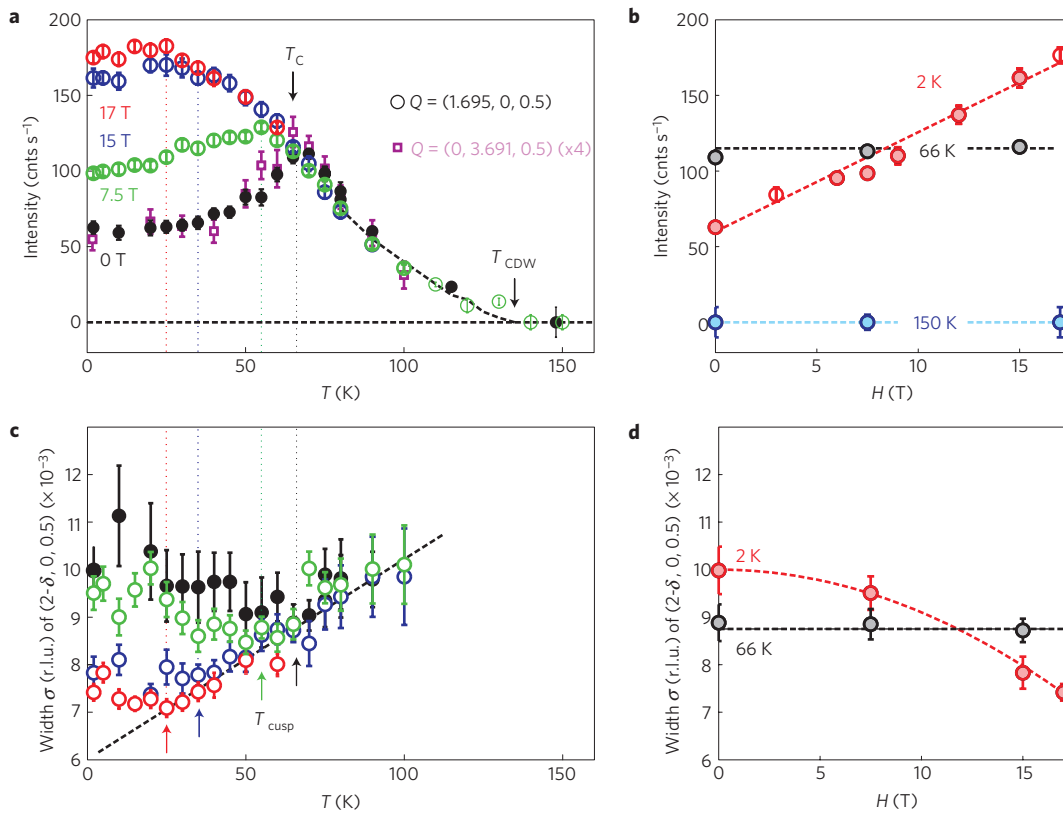


Figure 2 | Competition between charge-density-wave order and superconductivity. **a**, Temperature dependence of the peak intensity at (1.695, 0, 0.5) (circles) and (0, 3.691, 0.5) (squares) for different applied magnetic fields. The square data points have been multiplied by a factor of four. In the normal state, there is a smooth onset of the CDW order. In the absence of an applied magnetic field there is a decrease in the peak intensity below T_c . This trend can be reversed by the application of a magnetic field. **b**, Magnetic field dependence of the lattice modulation peak intensity at (1.695,0,0.5) for different temperatures. At $T = 2$ K, the peak intensity grows approximately linearly with magnetic field up to the highest applied field. **c,d**, Gaussian linewidth of the (1.695, 0, 0.5) CDW modulation plotted versus temperature and field respectively. The raw linewidth, including a contribution from the instrumental resolution, is field-independent in the normal state ($T > T_c$). In contrast, the CDW order becomes more coherent below T_c , once a magnetic field is applied. This effect ceases once the amplitude starts to be suppressed owing to competition with superconductivity. The vertical dashed lines in **a,c** illustrate the connection between these two features of the data that define the T_{cusp} temperatures. All other lines are guides to the eye. Error bars indicate standard deviations of the fit parameters described in Methods.

The intensities of the incommensurate Bragg peaks are sensitive to atomic displacements parallel to the total scattering vector \mathbf{Q} . The comparatively small contribution to \mathbf{Q} along the c^* direction from $l = 0.5$ r.l.u. means that our signal for a $(h, 0, 0.5)$ peak is dominated by displacements parallel to the a direction. (There will also be displacements parallel to the c direction but we are essentially insensitive to them in our present scattering geometry). Our data indicate that the incommensurate peaks are much stronger if they are satellites of strong Bragg peaks of the form $(\tau = (2n, 0, 0))$ at positions such as $\tau \pm \mathbf{q}_1$. This indicates that the satellites are caused by a modulation of the parent crystal structure. The fact that the scattering is peaked at $l = \pm 0.5$ r.l.u. means that neighbouring bilayers are modulated in antiphase. The two simplest structures (Fig. 3a,b) compatible with our data (see Supplementary Information) involve the neighbouring CuO_2 planes in the bilayer being displaced in the same (bilayer-centred) or opposite (chain-centred) directions, resulting in the maximum amplitude of the modulation being on the CuO_2 planes or CuO chains respectively. In their $2 - \mathbf{q}$ form, these structures would lead to the in-plane ‘checkerboard’ pattern shown in Fig. 3c. Scanning tunnelling microscopy studies of other underdoped cuprates¹⁶ and of field-induced CDW correlations in vortex cores¹⁷ also support the tendency towards checkerboard formation¹⁸, although disorder can cause small stripe domains to mimic checkerboard order¹⁹. Our observation of a CDW

may be related to phonon anomalies²⁰, which suggest that in YBCO near $p \approx 1/8$ there are anomalies in the underlying charge susceptibility for $\mathbf{q} \approx (0, 0.3)$.

Cuprate superconductors show strong spin correlations, and the interplay between spin and charge correlations may be at the heart of the high- T_c phenomenon. The spin correlations are largely dynamic, with energies up to several hundred meV. $\text{YBa}_2\text{Cu}_3\text{O}_{6+x}$ and $\text{La}_{2-x}(\text{Ba, Sr})_x\text{CuO}_{4+\delta}$ show incommensurate magnetic order, which can be enhanced by suppressing superconductivity with an applied magnetic field^{21–24}; this has some analogies with the CDW order observed here. The magnetic order is static on the ~ 1 meV frequency scale of neutron diffraction and has been detected in lightly doped $\text{YBa}_2\text{Cu}_3\text{O}_{6+x}$ for $p \leq 0.082$ (ref. 21), and moderately doped $\text{La}_{2-x}\text{Sr}_x\text{CuO}_4$ for $p \leq 0.14$ (ref. 24). The $\text{YBa}_2\text{Cu}_3\text{O}_{6.67}$ ($p \approx 1/8$) sample studied here is expected to have a relatively large spin gap, $\hbar\omega \approx 20$ meV (ref. 25), in its magnetic excitations at low temperature, making it unlikely that it orders magnetically. As discussed earlier, this is confirmed by other measurements^{13,14}, so the CDW does not seem to be accompanied by spin order. Moreover, there is no obvious relationship between \mathbf{q}_{CDW} and the wave vector of the incipient spin fluctuations $\mathbf{q}_{\text{SF}} \approx (0.1, 0)$ of similarly doped samples²⁵.

It is interesting to note that T_{CDW} corresponds approximately with T_{H} (Fig. 4), the temperature at which Hall effect measurements suggest that Fermi surface reconstruction begins²⁶. A CDW that

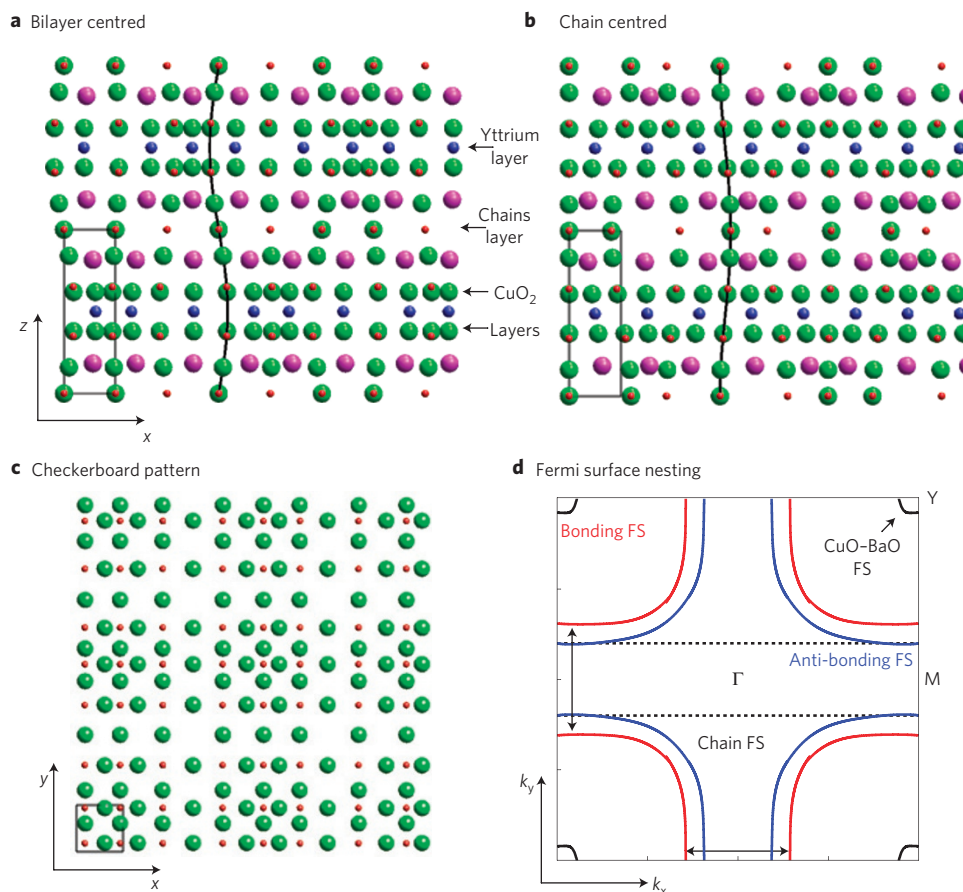


Figure 3 | Real space and reciprocal space pictures. **a,b**, One dimensional atomic displacements (exaggerated for clarity—the estimated amplitude is $\sim 0.003 \text{ \AA}$, see Supplementary Information) in the unit cell of YBCO ortho-VIII. The positions of yttrium (blue), barium (purple), copper (red) and oxygen (green) atoms are shown as a function of x (Cu–O bond direction) and z perpendicular to the CuO_2 planes. The structure in **a** has maximal displacement on the yttrium site and the displacement is the same in the two bilayer CuO_2 planes. In **b**, the structure has maximal displacement at CuO-chain positions and the displacement is opposite within the bilayer planes. Notice that the displacements in neighbouring bilayers are in anti-phase and the CuO chains are modulated with the ortho-VIII structure. **c**, Modulations along both Cu–O bond directions (x and y) lead to a checkerboard structure. **d**, Schematic of the Fermi surface (FS) of YBCO (based on ref. 28—see Supplementary Information). It consists of bonding (red) and anti-bonding (blue) sheets originating from the CuO_2 bilayer planes, one-dimensional open sheets from the oxygen chains and possible small pockets around the Y-point from the CuO–BaO layers. Coupling of the bonding states (indicated by vertical and horizontal arrows) favours the bilayer-centred structure, although this is in competition with intra-bilayer Coulomb effects (see Supplementary Information). Recent resonant X-ray scattering on an ortho-III sample also suggests that the CDW originates from the CuO_2 planes³². The arrows connecting the bonding bands near the zone boundary are compatible with the CDW vectors $\mathbf{q}_1 = (\delta_1, 0, 0.5)$ and $\mathbf{q}_2 = (0, \delta_2, 0.5)$ if the Fermi surface has a small dispersion along k_z .

breaks translational symmetry provides a natural mechanism for Fermi surface reconstruction and the formation of pockets. From the negative Hall and Seebeck coefficients^{10,11,26}, it was inferred that the Fermi pocket observed by quantum oscillations⁹ is electron-like¹⁰. The exact structure of the low-temperature reconstructed Fermi surface is still debated, although recent high-field specific heat experiments place constraints on the possibilities and suggest a small number of pockets²⁷ (see Supplementary Information). It is interesting to compare the LDA Fermi surface of YBCO (ref. 28) with \mathbf{q}_{CDW} (Fig. 3d and Supplementary Information). The electronic states most obviously connected by \mathbf{q}_{CDW} are the bonding bands at and near the zone boundary, which lie near the anti-nodal region of the superconducting gap, where the pseudogap is also maximized.

Our results have important implications for the phenomenology and phase diagram of the cuprates (Fig. 4). A simple Landau theory (see Supplementary Information) shows that T_c will be suppressed below the value it would have in the absence of the CDW. We speculate that this is reflected in the shape of the superconducting dome¹² (Fig. 4). One of the defining

properties of underdoped cuprates such as ortho-VIII YBCO is the pseudogap. This develops at the ‘crossover’ temperature T^* (for $\text{YBa}_2\text{Cu}_3\text{O}_{6.67}$, $T^* \approx 220 \text{ K}$), where there is a suppression of low-energy electronic states, evidence for ‘ $Q=0$ ’ magnetic order²⁹ and rotational anisotropy appears in various physical properties, such as the Nernst effect³⁰. The CDW reported here develops at $T_{\text{CDW}} \approx 135 \text{ K}$, inside the pseudogap state. From Fig. 2a,c we can identify the temperature $T_{\text{cusp}}(H)$ where the suppression of the CDW begins. The level of this competition indicates that the CDW and superconductivity have similar energy scales (10–30 meV), unlike NbSe_2 where the CDW order is not significantly suppressed by superconductivity⁴. $T_{\text{cusp}}(H)$ (Fig. 4) seems to correspond to the temperature $T_n(H)$ at which superconductivity in the mixed state can be identified from transport measurements rather than the appearance of zero resistance.

We draw attention to the situation in the cuprates that many different kinds of order, such as superconductivity, pseudogap, CDW and antiferromagnetism, occur on comparable temperature scales. When they compete, they do so on an almost equal footing. We may suspect that this is not accidental, and that

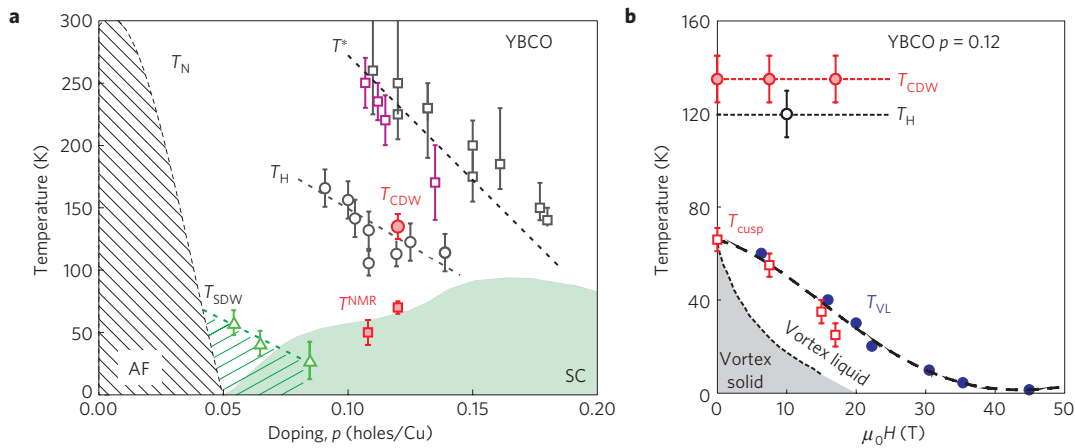


Figure 4 | Phase diagram of $\text{YBa}_2\text{Cu}_3\text{O}_{7-x}$. **a**, Doping dependence of the antiferromagnetic ordering temperature T_N , the incommensurate spin-density wave order T_{SDW} (green triangles; ref. 21), the superconducting temperature T_c and the pseudogap temperature T^* as determined from the Nernst effect³⁰ (black squares) and neutron diffraction²⁹ (purple squares). Notice that the Nernst effect³⁰ indicates a broken rotational symmetry inside the pseudogap region, whereas a translational symmetry preserving magnetic order is found by neutron scattering²⁹. Below temperature scale T_H (black circles), a larger and negative Hall coefficient was observed²⁶ and interpreted in terms of a Fermi surface reconstruction. Our X-ray diffraction experiments show that in $\text{YBCO } p = 0.12$ incommensurate CDW order spontaneously breaks the crystal translational symmetry at a temperature T_{CDW} that is twice as large as T_c . T_{CDW} is also much larger than T^{NMR} (red squares), the temperature scale below which NMR observes field-induced charge order¹³. **b**, Field dependence of T_{CDW} (filled red circles) and T_{cusp} (open squares), the temperature below which the CDW is suppressed by superconductivity, compared with T_H (open black circle) and T_{VL} (filled blue circles), the temperature where the vortex liquid state forms²⁶. Error bars on T_{SDW} , T_H , T^{NMR} , and T^* are explained in refs 21,26,30,33. The error bars on T_{CDW} and T_{cusp} reflect the uncertainty in determining the onset and suppression temperature of CDW order from Fig. 2.

these various orders are ‘intertwined’³¹. In this context, we can view our present results as indicating that the electron system has a tendency towards two ground states: a charge density wave, which breaks translational symmetry and involves electron–hole correlations, versus superconductivity, which breaks gauge symmetry and involves electron–electron correlations. We note that the \mathbf{q} -vectors of the CDW lie close to the separation of pieces of Fermi surface that have maximum superconducting gap at optimal doping and have the same sign of the order parameter.

Methods

Our experiments used 100 keV hard X-ray synchrotron radiation from the DORIS-III storage ring at DESY, Hamburg, Germany. We installed a recently developed 17 T horizontal cryomagnet designed for beamline use on the triple-axis diffractometer at beamline BW5. The sample was mounted by gluing it over a hole in a temperature-controlled aluminium plate within the cryomagnet vacuum and was thermally shielded by thin Al and aluminized mylar foils glued to this plate. The sample temperature could be controlled over the range ~ 2 –300 K. The incoming and outgoing beams passed through 1 mm thick aluminium cryostat vacuum windows, which gave a maximum of $\sim \pm 10^\circ$ input and output angles relative to the field direction, which was parallel to the sample c axis within $< 1^\circ$. Between the beam access windows and the sample plate, there were further aluminium foil thermal radiation shields at liquid nitrogen temperature. A 2 mm square aperture collimated the incoming beam, so that it passed mainly through the part of the sample over the hole in the aluminium plate, greatly reducing background scattering by the plate. Further slits before the analyser and the detector removed scattering by the cryostat windows and nitrogen shields. The scattering plane (a^*c^*) was horizontal. The cryomagnet was mounted on a rotation stage with a goniometer giving χ tilt about the field axis. The sample was initially mounted with its a axis nearly horizontal. The χ goniometer allowed the exact alignment of this axis using the $(2\ 0\ 0)$ Bragg peak and could also be used for low-resolution scans in the b^* direction. Magnetic fields were applied with the sample heated above T_c ; it was then field-cooled to base temperature. When fields were applied, minor changes in the position and angle of the sample holder were observed; these were corrected by use of horizontal and vertical motion stages under the cryostat rotation stage, and by realigning on the $(2\ 0\ 0)$ Bragg peak. During temperature scans, realignment on the $(2\ 0\ 0)$ Bragg peak was performed automatically at every temperature point to ensure that all measurements were centred. After results had been obtained with the a axis horizontal, the sample was remounted with the b axis horizontal for further measurements. The $\text{YBa}_2\text{Cu}_3\text{O}_{6.67}$ sample had dimensions $a \times b \times c = 3.1 \times 1.7 \times 0.6$ mm³ and mass 18 mg. The superconducting transition temperature $T_c = 67$ K (width: 10%–90% = 1.1 K) was derived from a zero-field-cooled magnetization curve at 0.1 mT. The single crystal was 99%

detwinned and the Cu–O chains were ordered with the ortho-VIII structure by standard procedures¹².

The diffracted intensities from the CDW, shown in Fig. 1, are composed of an incommensurate lattice modulation peak on a smoothly varying background. The background along $(h, 0, 0.5)$ mainly originates from the tails of the ortho-VIII peaks (see Supplementary Information). It varies strongly from one Brillouin zone to another; for example, the background around $(2.7, 0, 0.5)$ is an order of magnitude larger than around $(1.7, 0, 0.5)$. The background has essentially no field dependence (Fig. 1a–c) so subtracting the zero-field from high-field data is a simple way to eliminate the background. This reveals the field-enhanced signal inside the superconducting state (Fig. 1a–d).

As there is a weak temperature dependence in the background (Fig. 1a–c), it is not possible to eliminate it by subtracting a high-temperature curve. Therefore, to obtain the temperature dependences shown in Fig. 2, we fitted the data to a Gaussian function $G(Q)$ and modelled the background by a second-order polynomial $B(Q) = c_0 + c_1Q + c_2Q^2$. The constants c_0 , c_1 and c_2 have a small but significant temperature dependence. The low counting statistics resulted in Gaussians fitting equally well as other possible lineshapes such as Lorentzians.

The signal-to-background ratio is best for the $(2 - \delta_1, 0, 0.5)$ peak due to the weaker structural ortho-VIII peak (see Supplementary Fig. S2). From the Gaussian fits to the $(2 - \delta_1, 0, 0.5)$ satellite peak at 2 K and 17 T we can estimate the correlation length ξ along the three crystal axis directions. We define $\xi = 1/\sigma$, where $\sigma = (\sigma_{\text{mes}}^2 - \sigma_{\text{R}}^2)^{0.5}$ is the measured Gaussian standard deviation corrected for the instrument resolution σ_{R} and expressed in \AA^{-1} . Along the a axis direction, we find $\sigma = 6.4 \times 10^{-3}$ r.l.u. $\equiv 1.1 \times 10^{-2}$ \AA^{-1} , and hence $\xi_a = 95 \pm 5$ \AA . Deconvolving the poor instrumental resolution along the b axis direction for the $(2 - \delta_1, 0, 0.5)$ peak yields a similar correlation length $\xi_b \sim \xi_a$.

Received 18 June 2012; accepted 18 September 2012;
published online 14 October 2012

References

- Mathur, N. D. *et al.* Magnetically mediated superconductivity in heavy fermion compounds. *Nature* **394**, 39–43 (1998).
- Kivelson, S. A. *et al.* How to detect fluctuating stripes in the high-temperature superconductors. *Rev. Mod. Phys.* **75**, 1201–1241 (2003).
- Vojta, M. Lattice symmetry breaking in cuprate superconductors: Stripes, nematics, and superconductivity. *Adv. Phys.* **58**, 699–820 (2009).
- Moncton, D. E., Axe, J. D. & DiSalvo, F. J. Neutron scattering study of the charge–density wave transitions in 2H-TaSe_2 and 2H-NbSe_2 . *Phys. Rev. B* **16**, 801–819 (1977).
- Demler, E., Sachdev, S. & Zhang, Y. Spin-ordering quantum transitions of superconductors in a magnetic field. *Phys. Rev. Lett.* **87**, 067202 (2001).
- Tranquada, J. M. *et al.* Evidence for stripe correlations of spins and holes in copper oxide superconductors. *Nature* **375**, 561–563 (1995).

7. Fujita, M., Goka, H., Yamada, K., Tranquada, J. M. & Regnault, L. P. Stripe order, depinning, and fluctuations in $\text{La}_{1.875}\text{Ba}_{0.125}\text{CuO}_4$ and $\text{La}_{1.875}\text{Ba}_{0.075}\text{Sr}_{0.05}\text{CuO}_4$. *Phys. Rev. B* **70**, 104517 (2004).
8. Von Zimmermann, M. *et al.* Oxygen-ordering superstructures in underdoped $\text{YBa}_2\text{Cu}_3\text{O}_{6+x}$ studied by hard x-ray diffraction. *Phys. Rev. B* **68**, 104515 (2003).
9. Doiron-Leyraud, N. *et al.* Quantum oscillations and the Fermi surface in an underdoped high- T_c superconductor. *Nature* **447**, 565–568 (2007).
10. LeBoeuf, D. *et al.* Electron pockets in the Fermi surface of hole-doped high- T_c superconductors. *Nature* **450**, 533–536 (2007).
11. Laliberté, F. *et al.* Fermi-surface reconstruction by stripe order in cuprate superconductors. *Nature Commun.* **2**, 432 (2011).
12. Liang, R. *et al.* Evaluation of CuO_2 plane hole doping in $\text{YBa}_2\text{Cu}_3\text{O}_{6+x}$ single crystals. *Phys. Rev. B* **73**, 180505 (2006).
13. Wu, T. *et al.* Magnetic-field-induced charge-stripe order in the high-temperature superconductor $\text{YBa}_2\text{Cu}_3\text{O}_y$. *Nature* **477**, 191–194 (2011).
14. Ghiringhelli, G. *et al.* Long-range incommensurate charge fluctuations in $(\text{Y}, \text{Nd})\text{Ba}_2\text{Cu}_3\text{O}_{6+x}$. *Science* **337**, 821–825 (2012).
15. Abbamonte, P. Charge modulations versus strain waves in resonant x-ray scattering. *Phys. Rev. B* **74**, 195113 (2006).
16. Schmidt, A. R. *et al.* Electronic structure of the cuprate superconducting and pseudogap phases from spectroscopic imaging. *New J. Phys.* **13**, 065014 (2011).
17. Hoffman, J. E. *et al.* A four unit cell periodic pattern of quasi-particle states surrounding vortex cores in $\text{Bi}_2\text{Sr}_2\text{CaCu}_2\text{O}_{8+\delta}$. *Science* **295**, 466–469 (2002).
18. Wise, W. D. *et al.* Charge-density-wave origin of cuprate checkerboard visualized by scanning tunnelling microscopy. *Nature Phys.* **4**, 696–699 (2008).
19. Robertson, J. A. *et al.* Distinguishing patterns of charge order: Stripes or checkerboards. *Phys. Rev. B* **74**, 134507 (2006).
20. Reznik, D. *et al.* Electron-phonon coupling reflecting dynamic charge inhomogeneity in copper oxide superconductors. *Nature* **440**, 1170–1173 (2006).
21. Haug, D. *et al.* Neutron scattering study of the magnetic phase diagram of underdoped $\text{YBa}_2\text{Cu}_3\text{O}_{6+x}$. *New J. Phys.* **12**, 105006 (2010).
22. Lake, B. *et al.* Antiferromagnetic order induced by an applied magnetic field in a high-temperature superconductor. *Nature* **415**, 299–302 (2002).
23. Khaykovich, B. *et al.* Enhancement of long-range magnetic order by magnetic field in superconducting $\text{La}_2\text{CuO}_{4+y}$. *Phys. Rev. B* **66**, 014528 (2002).
24. Chang, J. *et al.* Tuning competing orders in $\text{La}_{2-x}\text{Sr}_x\text{CuO}_4$ cuprate superconductors by the application of an external magnetic field. *Phys. Rev. B* **78**, 104525 (2008).
25. Dai, P., Mook, H. A., Hunt, R. D. & Dogan, F. Evolution of the resonance and incommensurate spin fluctuations in superconducting $\text{YBa}_2\text{Cu}_3\text{O}_{6+x}$. *Phys. Rev. B* **63**, 054525 (2001).
26. LeBoeuf, D. *et al.* Lifshitz critical point in the cuprate superconductor $\text{YBa}_2\text{Cu}_3\text{O}_y$ from high-field Hall effect measurements. *Phys. Rev. B* **83**, 054506 (2011).
27. Riggs, S. C. *et al.* Heat capacity through the magnetic-field-induced resistive transition in an underdoped high-temperature superconductor. *Nature Phys.* **7**, 332–335 (2011).
28. Carrington, A. & Yelland, E. A. Band-structure calculations of Fermi-surface pockets in ortho-II $\text{YBa}_2\text{Cu}_3\text{O}_{6.5}$. *Phys. Rev. B* **76**, 140508 (2007).
29. Li, Y. *et al.* Unusual magnetic order in the pseudogap region of the superconductor $\text{HgBa}_2\text{CuO}_{4+\delta}$. *Nature* **455**, 372–375 (2008).
30. Daou, R. *et al.* Broken rotational symmetry in the pseudogap phase of a high- T_c superconductor. *Nature* **463**, 519–522 (2010).
31. Berg, E., Fradkin, E., Kivelson, S. A. & Tranquada, J. M. Striped superconductors: How spin, charge and superconducting orders intertwine in the cuprates. *New J. Phys.* **11**, 115004 (2009).
32. Achkar, A. J. *et al.* Distinct charge orders in the planes and chains of ortho-III ordered $\text{YBa}_2\text{Cu}_3\text{O}_{6+\delta}$ identified by resonant elastic x-ray scattering. Preprint at <http://arxiv.org/abs/1207.3667>.
33. Chang, J. *et al.* Nernst effect in the cuprate superconductor $\text{YBa}_2\text{Cu}_3\text{O}_y$: Broken rotational and translational symmetries. *Phys. Rev. B* **84**, 014507 (2011).

Acknowledgements

We thank B. L. Gyorffy, M. W. Long, J. A. Wilson, A. J. Schofield, J. R. Cooper, J. W. Loram, S. A. Kivelson, L. Taillefer, C. Bourbonnais, C. Proust and A. Kapitulnik for discussions and R. Nowak, G. R. Walsh and J. Blume for technical assistance. This work was supported by the EPSRC (grant numbers EP/G027161/1 and EP/J015423/1), the Wolfson Foundation, the Royal Society, the Danish Agency for Science, Technology and Innovation under DANSCATT and the Swiss National Science Foundation through NCCR-MaNEP and grant number PZ00P2_142434. J.C., N.B.C. and J.M. are grateful to L. Braicovich, G. Ghiringhelli, B. Keimer and M. Le Tacon for communicating their results to them after this experiment was completed.

Author contributions

D.A.B., W.N.H. and R.L., prepared the samples. E.B., J.C., N.B.C., E.M.F., S.M.H., M.v.Z. and A.W. conceived and planned the experiment. E.B., J.C., N.B.C., E.M.F., S.M.H., A.T.H., J.L. and M.v.Z. carried out the experiment. J.C., E.M.F. and S.M.H. carried out data analysis and modelling. E.B., J.C., N.B.C., E.M.F. and S.M.H. wrote the paper. J. M. was responsible for research direction and planning at PSI. All authors discussed the results and commented on the manuscript.

Additional information

Supplementary information is available in the online version of the paper. Reprints and permissions information is available online at www.nature.com/reprints. Correspondence and requests for materials should be addressed to J.C.

Competing financial interests

The authors declare no competing financial interests.